IEEE Access
Multidisciplinary ⋮ Rapid Review ⋮ Open Access Journal

Received December 9, 2020, accepted December 20, 2020, date of publication December 24, 2020,
date of current version January 11, 2021.

Digital Object Identifier 10.1109/ACCESS.2020.3047110

A MOSFET SPICE Model With Integrated Electro-Thermal Averaged Modeling, Aging, and Lifetime Estimation

TIAN CHENG, (Student Member, IEEE), DYLAN DAH-CHUAN LU, (Senior Member, IEEE), AND YAM P. SIWAKOTI, (Senior Member, IEEE)
School of Electrical and Data Engineering, University of Technology Sydney, Sydney, NSW 2007, Australia

Corresponding author: Tian Cheng (tian.cheng@student.uts.edu.au)

This work was supported in part by the Australian Government through the Australian Research Council under Discovery Project DP180100129.

ABSTRACT Lifetime estimation of power semiconductor devices have been widely investigated to improve the reliability and reduce the cost of maintenance of power converters. However in most reported work, the aging effect is not considered in the lifetime evaluation process due to the omission or limitation of thermal cycle counting method. Additionally, the electrical/thermal simulation and lifetime estimation are usually implemented in different simulators/platforms, for the same reason. Thus, to tackle these problems, a concise but comprehensive MOSFET model that enables electro-thermal modeling, aging and lifetime estimation on LTspice®circuit simulator is proposed in this paper. The idea comes from the fact that, MOSFET on-state resistance $R_{ds,on}$ is not only temperature dependent, but also widely accepted as the device failure precursor. In other words, as it carries critical information about instantaneous temperature and aging progress. Hence, co-simulation can be achieved by constructing electrical, thermal, and aging and lifetime sub-modules exclusively first, and using $R_{ds,on}$, to build linkages among them. Averaged modeling technique is adopted due to the ease of establishing links among these three sub-modules, and fast simulation speed as compared to a switched converter model. Behavioral models are employed to realize the thermal cycles counting, stress accumulation and degradation evaluation. This paper demonstrates that it is possible to use a single simulation software to monitor performances of devices and circuits, and their lifetime estimation simultaneously. High-stress thermal cycling and long-term random mission profiles are applied to verify the correctness of the model and to mimic a 10-year load respectively. An accelerated aging trend can be observed in the long-term mission profile simulation, which is in agreement with the theory. Facilitated by the employment of averaged circuits, the proposed method is a good simulation/analytical tool to implement a long-term mission profile that requires reliability assessment.

INDEX TERMS MOSFET model, lifetime estimation, degradation, electro-thermal averaged model, LTspice simulation.

I. INTRODUCTION

Reliability is one of the most challenging factors that needs thorough consideration when designing converters/inverters. It is especially critical for those devices which require to carry out challenging mission profiles while operating in severe environmental conditions. In addition, it has also attracted attention to future power supply design with increasing power density requirement. To avoid the downtime of power supplies and any catastrophic failures both electrically and economically, reliability assessment and prediction of useful lifetime of power devices are widely investigated. By knowing the effective operation duration of devices, maintenance can be scheduled before the device fails. Hence, the reliability of the circuits and systems can be greatly improved, and the maintenance cost can be saved.

Recent research works focusing on device reliability and lifetime evaluation are reviewed. In [1], an experimental platform which allows concurrent execution of accelerated thermal cycling tests on multiple MOSFETs is built for

The associate editor coordinating the review of this manuscript and approving it for publication was Xiao-Sheng Si.

reliability assessment. In [2], a MOSFET reliability model is proposed to predict $R_{ds,on}$ parametric drift through analyzing temperature distribution on the source metal so that the degree of degradation and lifetime of the MOSFET can be estimated. Experimental-based or endurance tests are traditional methods in assessing devices performance. They are reliable however the process is very time consuming. Long term and intensive tests are usually needed. Based on the device-level studies, lifetime descriptive model can be derived and they are widely employed in evaluating the lifetime of converters/inverters [3]–[13]. In [3], a fast lifetime prediction simulation strategy based on conditions mapping (ambient temperature and load) and look-up tables (losses, junction temperature and load) is proposed for a SiC power module used in a PV inverter topology. In [4], an evaluation of bond wire fatigue of IGBTs in a PV inverter under a long-term operation are given. In [5], the lifetime of T-type and I-type power modules employed in 1500-V three-level PV inverters with different mission profiles and operation frequencies are evaluated respectively. In [6], the study investigates both impacts of installation sites and the PV panel degradation rate on the lifetime of the PV inverters. In [7], a detailed wear-out failure probability analysis of a PV micro-inverter is presented aiming at identifying the weak point and improving the system reliability. In [8], the lifetime of a modular multilevel converter (MMC) with half-bridge as submodules operates in an offshore high voltage direct current offshore wind power system are studied. The impacts of comprehensive mission profiles on the lifetime of wind power converters are studied with an improved estimation method by considering different time scale thermal behaviors in [9]. Similarly, a comparative lifetime evaluation of several three-level converters with different modulation schemes are presented by simulating a 10-MW drivetrain [10]. In [11], the lifetime of a grid connected voltage source inverter is estimated, and a thermal resistance feedback system which reflects the device self-accelerating phenomenon is also introduced. In [12], an online evaluation of the consumed lifetime of a IGBT full bridge converter is presented through adopting the electro-thermal model, the physics-of-failure analysis and the real-time thermal counting algorithm. In [13], an online rainflow counting algorithm is also proposed to check the in-service operation of a three-level traction converter.

Although the aforementioned converters/inverters are applied to different applications in [3]–[13], they follow a similar lifetime estimation procedure: 1. Apply environment profiles (e.g. ambient temperature, wind speed, etc.) and load profiles into inverter/converter in the circuit simulation tool (e.g. PLECS, LTspice®, MATLAB, etc.), and get device junction temperature profile generated though electro-thermal model (ETM); 2. Input the temperature profile into a thermal cycle counting method to distribute the random cycles into different organized categories. The processed cycles information is utilized in the lifetime analytic model (e.g. Coffin-Manson law, etc.) and damage accumulation model to estimate the consumed and remaining lifetime. All the works in [3]–[13] have considered the device damage phenomenon, however, only [11]–[13] have included this degradation into lifetime estimation. Nevertheless, instantaneous updating of thermal resistance caused by aging is not allowed in [11] due to the application of offline rainflow counting algorithm. While method used in [12] suits more for real-time estimation as it used real-time data which contains aging information already. The problem of offline counting in [11] is solved in [13], however, this method rely more on programming, but difficult to be adopted in circuit simulators as the proposed online rainflow counting algorithm is stack based.

As the device aging progress is in an accelerated trend, inclusion or exclusion of this process will cause a significant difference in estimation results. The estimated lifetime values of IGBT which included and excluded aging process are 28.25 and 39.5 years respectively in [11]. In addition, it has also been pointed out that, the lifetime of an IGBT module not only is dependent on the stress level, but also on the current health state of a device [14], [15]. Therefore, it will be of great benefit if the aging parameters can be monitored in the modeling process. Moreover, most of the studies above investigate the aging effects on the lifetime of IGBTs, however, few of them has taken discrete MOSFETs into account, which are also widely used in current power supplies. As these two devices are applied to different power rating applications, different packages are used. For instance, widely evaluated IGBTs are of the module design for its capability of high currents handling, while for the MOSFETs, discrete package (e.g. TO220, TO247, etc.) are more common. For this reason, aging impacts on different parameters of these two devices, for example, thermal resistance of IGBT modules, and $R_{ds,on}$ of MOSFETs are considered. Noted that, the aging does affect the thermal resistance R_{th} of a MOSFET, and R_{th} can be used as the failure precursor too. However, as compared to the R_{th}, the advantages of using $R_{ds,on}$ as healthy indicator are due to its higher sensitivity and ease of accessibility [16]. Hence, the aging of $R_{ds,on}$ should be considered.

To tackle this problem and to provide an alternative solution on an open-source or freeware platform particularly, a MOSFET model which contains three sub models, namely, electro-thermal averaged model, aging model, and lifetime analytic model is proposed in this paper. Co-simulation of these three models and inclusion of aging effect can be achieved by forming feedback loops among MOSFET on-state resistance $R_{ds,on}$, junction temperature and accumulated stresses. While the lifetime of a device can be evaluated through assessing the degradation level or, in other words, the variation of the $R_{ds,on}$. Detailed derivation steps of this model are presented, and simulated results of both accelerated aging tests and long-term mission profile test are investigated and discussed.

II. DERIVATION PRINCIPLE OF THE PROPOSED MODEL

The aim of this work is to build a MOSFET SPICE model which can realize online simulation of electrical and thermal

performances, degradation and lifetime estimation simultaneously. To achieve the co-simulation in a single software, LTspice®, which is a free and powerful circuit simulation tool is selected in this paper. Since it focuses more on electrical domain simulation, transformation between thermal domain and electrical domain requires thermal-electrical analogy. The temperature (°C) and power loss (W) in the thermal domain are represented by a voltage source (V) and a behavioral current source (A) in the electrical domain respectively.

An overview of the model operation principle is shown in Fig. 1. An averaged circuit of a power converter, i.e. a boost converter is taken as an example, is adopted to achieve time-effective electrical simulation, while the device temperature can be easily estimated by constructing a resistor thermal network. Combining these two models together, a complete electro-thermal averaged model (ETAM) is formed. The lifetime analytic model and MOSFET degradation model are added with the help of behavioral models. Instead of using a fixed $R_{ds,on}$ value in the electrical model, a variable which is a function of its initial electrical characteristic, temperature and aging effects is used. Through this approach, the feedback loops between any two models are formed. The complete circuitry of the proposed MOSFET SPICE model developed in LTspice®is shown in Fig. 2, while the derivation principles of sub-models contained in the model are discussed as follows.

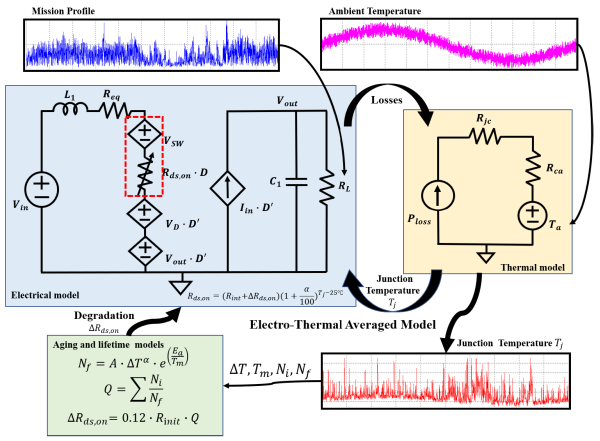

FIGURE 1. An overview of the proposed integrated electro-thermal averaged modeling, aging and lifetime model.

A. DERIVATION OF THE ELECTRO-THERMAL AVERAGED MODEL (ETAM)

The derivation and verification of the electro-thermal averaged model is based on the previous work developed in [17]. This model mainly contains an electrical model and a thermal model, and they are linked by utilizing the characteristic that the MOSFET $R_{ds,on}$ is temperature dependent.

1) ELECTRICAL MODEL

The derivation principle of the circuit is similar to the conventional averaged boost circuit. The inductor and diode series resistances are combined and represented by R_{eq}, V_D is the diode forward voltage drop, D and D' are namely the duty cycle and its inverse respectively. Additionally, two main modifications are made. First, the $R_{ds,on}$ is no longer a fixed value but is temperature and aging dependent. The value can be estimated by (1), in which, R_{init}, T_j, $\Delta R_{ds,on}$, and α indicate the initial $R_{ds,on}$ value, MOSFET junction temperature, degradation caused increment of resistance $\Delta R_{ds,on}$ and coefficient respectively. Two factors that contribute to the increase of T_j are conduction losses and switching losses. As the averaged model is switching frequency independent, while the switching losses play a significant role especially at a high frequency, the second modification is to induce the switching losses effects into the averaged model. The losses can be calculated by using (2), where the term f_s, T_r, T_f, I_{in}, V_{out} indicate the converter operation frequency, MOSFET turn-on rise time, turn-off fall time, input current, and the output voltage respectively. The switching losses can be represented by using an extra equivalent variable resistor ($R_{sw} = P_{sw}/I_{in}^2$) in the circuit. Alternatively, a simple extra voltage source V_{sw} by using (3) can be added as a result of (2), and the calculation steps can be saved. Regarding the conduction losses, it can be easily calculated by (4), where $i_{m_{rms}}$ is MOSFET RMS current. The losses will be input into the thermal model.

$$R_{ds,on} = (R_{init} + \Delta R_{ds,on}) \cdot (1 + \frac{\alpha}{100})^{T_j - 25°C} \quad (1)$$

$$P_{sw} = 0.5 \cdot f_s \cdot (T_r + T_f) \cdot V_{out} \cdot I_{in} \quad (2)$$

$$V_{sw} = 0.5 \cdot f_s \cdot (T_r + T_f) \cdot V_{out} \quad (3)$$

$$P_{cond} = i_{m_{rms}}^2 \cdot R_{ds,on} \cdot D \quad (4)$$

2) THERMAL MODEL

A simple thermal model is formed by injecting power losses into a resistance network. Both switching and conduction losses represented by two behavioral current sources PL_SW and PL_Ron are considered in Fig. 2, and input into two thermal resistances, namely, junction to case R_{jc}, case to ambient R_{ca} of MOSFET. Noted that, since the averaged model considers the steady state operation, thus, instead of using conventional RC foster or cauer thermal network, only R is considered here. The T_a represented by a voltage source is the ambient temperature. In simulation, a constant temperature is used for the accelerated tests. While for the long-term mission profile simulation, T_a, which composed of daily and annually information with some noises is adopted, to mimic a more realistic environment profile. It is made by merging two sine waves with some randomly generated noises. Alternatively, it can be achieved by importing a real environment profile.

B. DERIVATION OF LIFETIME ANALYTICAL MODEL AND AGING MODEL

In addition to its temperature-dependent characteristic of MOSFET $R_{ds,on}$, it is also widely accepted as a device failure precursor. In other words, $R_{ds,on}$ contains device degradation information too. Thus, advantage can be taken by adding the

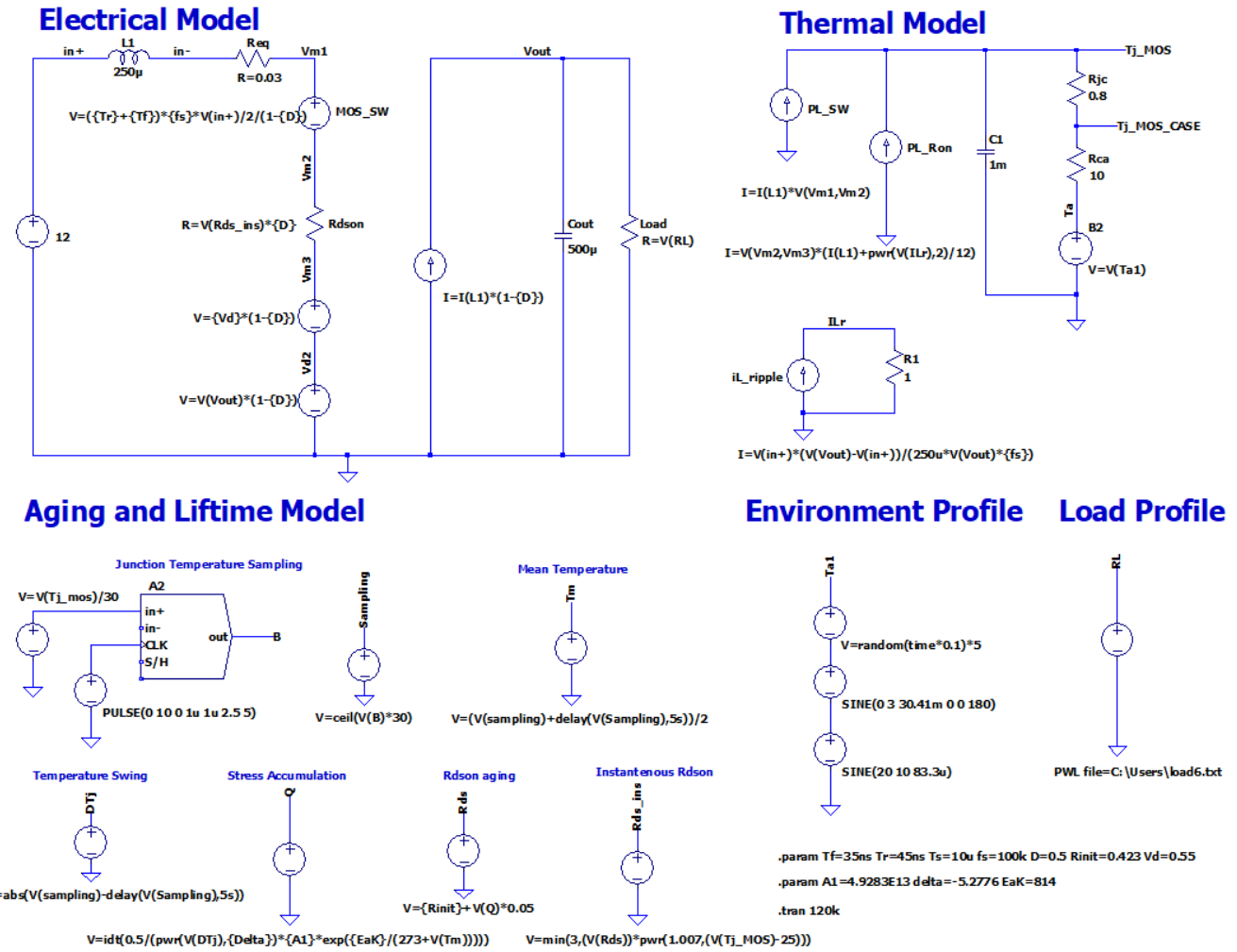

FIGURE 2. The detailed circuitry of the proposed integrated electro-thermal average model, aging and lifetime model developed in LTspice®.

degradation effects into the derived ETAM. Another benefit of employing the averaged circuit over the switching-mode circuit is that, it is well suited for simulating long-term mission profile due to its fast simulation speed.

1) LIFETIME ANALYTICAL MODEL

In order to evaluate the lifetime of MOSFET, the widely accepted Coffin-Manson law (5) is adopted to evaluate the device failure cycles. Parameters N_f, ΔT_j, T_m, E_a and k are namely, number of cycles before a device generates a fault under certain thermal stress, junction temperature swing, mean temperature, thermal activation energy and Boltzman constant respectively, while δ and A_1 are empirical coefficients. Another important factor in lifetime estimation is the accumulated stress Q, which evaluates the stress that a device has undertaken after a number of thermal cycles. Widely adopted method to calculate it is by using the Miner's rule (6), where N_i indicates the cycles a device has performed. Once the Q value reaches one, the threshold of the end-of-useful lifetime of a device is reached. Thus, a continuous and linear accumulation of Q can be observed.

To calculate the above two equations, it is necessary to count thermal cycles and to collect the ΔT_j and T_m data in each cycle. Counting algorithms, such as, half-cycle, maximum-edge, and the rainflow counting methods are widely adopted and compared [20]. The rainflow counting method is the most popular one with high accuracy. However, it usually needs to be applied offline as a complete thermal profile is required. Therefore it is not suitable to implement as an online algorithm in circuit simulation. In this paper, the half-cycle peak through counting method which counts the cycle rising and falling slope as 2 half cycles is adopted. The detailed operation in simulation is to compare the T_j amplitude of the current thermal cycle to the previous one, and generate the difference ΔT_j and mean temperature T_m curves. The values are fed back to (5) and (6), and counted as half cycle.

$$N_f = \Delta T_j^{\delta} A_1 e^{\frac{E_a}{kT_m}} \tag{5}$$

$$Q = \sum_{i=1}^{n} \frac{N_i}{N_f} \tag{6}$$

2) AGING MODEL

An aging model is included in this work to compensate the Miner's rule, as the linear stress accumulation can hardly reflect the self-accelerating degradation process [11]. A stress feedback model and a non-linear stress accumulation model are proposed in [11] and [21] respectively to reflect the IGBT degradation performances. In this paper, the feedback method is adopted, since the nonlinear method suits more for the IGBT thermal resistance failure mechanism which has a long crack initiation stages but will be propagated fast after reaching a certain limit. While for MOSFETs, although the aging is similarly in an exponential trend, the growing is not as steep as IGBT. Based on the study in [1] and [2], the aging of MOSFETs can be observed through monitoring the increment of $R_{ds,on}$. Two different models are proposed by them to represent this phenomenon.

In [1], an exponential degradation model represented by (7) is proposed based on the experimental results, as shown in Fig. 3, where α and β are coefficients which can be obtained through using curve fitting tool, and R_{init} is the initial $R_{ds,on}$ value. Therefore, the incremental $\Delta R_{ds,on} = \alpha e^{\beta t}$.

$$R_{ds,on}(t) = \alpha e^{\beta t} + R_{init} \tag{7}$$

Since this model is derived from experimental results, a direct deployment as such can effectively depict the degradation of the device. However, different stresses will give different degradation performances, which will result in different α and β values. In other words, one group of α and β values is only suitable for a certain stress operation. This will bring difficulties in calculating the accumulated stress when a practical mission profile is applied.

To solve this problem, a Remaining Useful Lifetime (RUL) estimation method is proposed in [19] through using Kalman filter and online computation to continuously update these two values. A random sample consensus (RANSAC) algorithm coupled with a sliding window method are proposed in [22] to delete outliers and to track some nonlinear samples in the experiment data respectively to improve the RUL estimation accuracy. These two methods focus on improving the accuracy of predicting the aging growing trend or failures on real data sets, as they are capable of dealing with sampling noises, hence, they are more suitable for real-time prognosis.

In this paper, a straightforward approach to approximate α and β values is proposed to give a general estimation. By taking the natural logarithm of both sides of $\Delta R_{ds,on} = \alpha e^{\beta t}$, it produces (8). A linear equation can be obtained, where t represents N_i cycles, β is the slope and α is the initial value. To verify this, degradation data points of cases (A)-(C) in Fig. 3 are extracted, and the α and β values are obtained through curve fitting. Following (8), the sample points are replotted in Fig. 4, which all three cases show almost linear growing trend. Another thing that worth noticing is that, the initial increments of $\Delta R_{ds,on}$ remain small for all devices under different stress levels. This can be observed from both Figs. 3 and 4, where the $\ln(\Delta R_{ds,on})$ ranges from -7 to -6, which is equivalent to 0.00091 to 0.00245. The range may contain small mismatches as compared to the real experimental results due to extraction errors, however, it still gives an insight into the estimation. Hence, an assumption is made that a small and fixed α value 0.0015 which is when $\ln(\Delta R_{ds,on}) = -6.5$ is applied to all cycles, such that, the β can be easily calculated by taking the preset maximum allowed $\Delta R_{ds,on}$ value, N_f for a certain stress into the equation. Both of the curve fitted α, β values and the calculated ones are shown in Table 2, together with its corresponding N_f cycles.

$$\ln(\Delta R_{ds,on}) = \ln(\alpha) + \beta t \tag{8}$$

In [2], the authors point out that the variation of $\Delta R_{ds,on}$ can be related to the accumulated stress Q. A maximum $\Delta R_{ds,on}$ of 0.2 p.u. of its initial $R_{ds,on}$ is set as the upper limit of a device before it is actually failed. Hence, the development of stress related aging model can be represented by (9).

$$\Delta R_{ds,on} = 0.2 \cdot R_{init} \cdot \sum_{i=1}^{n} \frac{N_i}{N_f} = 0.2 \cdot R_{init} \cdot Q \tag{9}$$

As discussed above, coefficients in the exponential equation may differ from one to another due to different stresses. In contrast, this approach gives a more simple and general solution as it is stress related.

All of these three aging models, namely, the exponential degradation model proposed by [1], the modified exponential model by authors, and the stress related model by [2] will be evaluated and discussed in Section III.

C. DESCRIPTION OF LTspice® FUNCTIONS USED IN THE CIRCUIT

A few functions employed in the behavioral current or voltage sources are explained in Table 1, and the description can be found from [18]. Another special symbol A2 adopted in the aging and lifetime model is the sample and hold function. Due to the maximum allowed sample voltage, which is 10 V, the MOSFET junction temperature needs to be scaled down before input to this function. It can be converted back to its original value by using the behavioral source.

TABLE 1. Description and explanation of LTspice® Functions used in the proposed model.

Function	Description [18]	Purposes of these functions in the model
ceil(x)	Integer equal or greater than x	filter out fraction for ease of calculation
min(x,y)	The smaller of x or y	limit $R_{ds,on}$
idt(x)	Integrate x	accumulate stresses
random(x)	Random number between [0,1]	generate noises
delay(x,t)	x delayed by t	generate a waveform with t cycles delayed for comparison
abs(x)	Absolute value of x	calculate ΔT_j

III. SIMULATION RESULTS

In this section, simulation results of the proposed MOSFET model with high stress thermal cycling mission profiles and a long-term random one are given. As the authors have provided very detailed experimental results and explanations in [19] based on the experimental platform built in [1], hence, in this work, the same MOSFET model IRFP340 with initial R_{init} at 0.423 ohm is used. Following this work, the degradation limit of $\Delta R_{ds,on}$ is set to 0.12 p.u. instead of 0.2 p.u., which is equivalent to 50 mΩ. The values of parameters V_{in}, f_s, D, R_{eq}, and V_D in the open-loop converter operation are 12V, 100 kHz, 0.5, 0.03 ohm and 0.55V respectively.

A. HIGH STRESS THERMAL CYCLING MISSION PROFILE

To verify the correctness of the proposed model, mission profiles which mimic the high stress thermal cycling experiments done in [19] is applied to the model first. Four cases are simulated here, A) $\Delta T = 160$ °C, $T_m = 160$°C, B) $\Delta T = 140$°C, $T_m = 140$°C, C) $\Delta T = 130$°C, $T_m = 145$°C, and D) $\Delta T = 80$°C, $T_m = 120$°C. A simple electrical circuit is adopted here to achieve the thermal cycling simulation, by using a DC voltage source in series with the MOSFET $R_{ds,on}$ and a pulsating load. Only conduction losses need to be considered in this simulation and the pulsating load allows the device to reach the desired temperature swing ΔT and mean temperature T_m easily. The thermal and lifetime submodules remain unchanged. A constant ambient temperature $T_a = 25$°C is assumed for all four cases in the simulation. Part of experimental results of cases (A) to (D) from [19] are replotted in Fig. 3, where multiple groups of testing results of cases (A) and (D) are given, while a single group of result of cases (B) and (C) is provided respectively. Noted that, due to the small discrepancies of devices in manufacture settings, degradation performances of devices differ from one to another. This can be observed from the experimental results of both cases (A) and (D). Hence, selected experimental results are used to derive the coefficients δ and A_1 in (5), which are -5.2776 and 4.9283×10^{13} respectively given in [19]. Hence, the calculated N_f based on Coffin–Manson model (5) for above four cases are namely, 750, 1586, 2410, and 35200 cycles. Selected experimental results of cases (A)-(D) are R_{6a}, R_{1a}, R_{2a}, and R_{8b} from Fig. 3 respectively, as they match the calculated N_f better.

To give an overview evaluation of the proposed model which embeds with the aforementioned three different aging models respectively, the N_f results of cases (A)-(D) of them are summarized and compared in Table 2. As can be observed, for the exponential model proposed by [1], since this model is based on the experimental results, where α_1 and β_1 values are extracted through curve fitting these devices aging waveforms, this method allows an effectively depiction of the aging of a device. For the exponential aging with the proposed α_2 and β_2 values, the simulated N_f fits the calculated N_f more for all cases as compared to the experimental results. It is because β_2 is obtained from the calculated N_f value. Hence, a conclusion can be made that, the accuracy of this method is

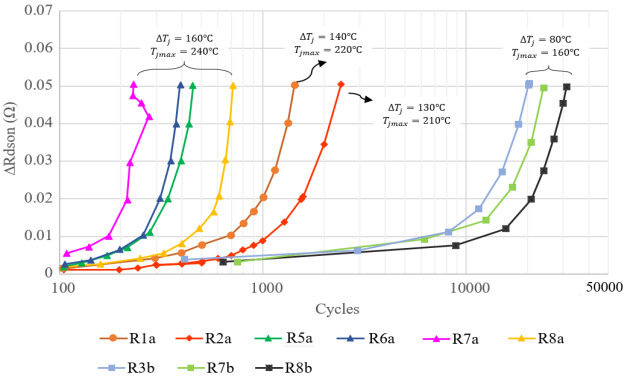

FIGURE 3. Replotted experimental results from [19] of online $\Delta R_{ds,on}$ monitoring during thermal cycling under three different conditions: (A) $\Delta T_j = 160$ °C, $T_{max} = 240$°C (R5a-R8a) (B) $\Delta T_j = 140$°C, $T_{max} = 220$°C (R1a), (C) $\Delta T_j = 130$°C, $T_{max} = 210$°C (R2a), and (D) $\Delta T = 80$°C, $T_m = 120$°C (R3b, R7b and R8b).

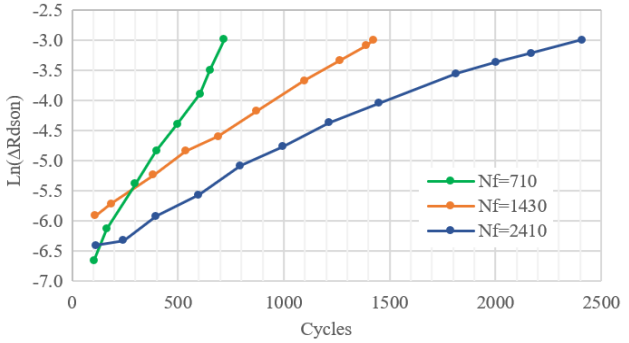

FIGURE 4. Natural logarithm plot of $\Delta R_{ds,on} = \alpha e^{\beta t}$ with the N_f for cases: (A) $\Delta T_j = 160$ °C, $T_{max} = 240$°C, (B) $\Delta T_j = 140$°C, $T_{max} = 220$°C, and (C) $\Delta T_j = 130$°C, $T_{max} = 210$°C.

in relation to the precision of N_f lifetime analytical models. While for the stress related model, it gives closer to the experimental results in most cases. However, a relatively bigger error in terms of the aging trend will occur in the high stress thermal cycling simulation as can be observed from Fig. 5, for example, maximum of 15 mΩ error can be found in case (A). Nevertheless, the error can be minimized in the long-term mission profile simulation, as to reach the maximum limit it needs hundreds of thousands of cycles. This conclusion can be found from observing case (A) to case (D). With the increase of N_f cycles, mismatches between simulation and experiments are reduced, from maximum of 15 mΩ to around 8 mΩ. Since, in relatively low stressed (e.g. case (D)) thermal cycling experiments, both the exponential and the stress related description models give flat growing trends. In other words, the stress related model will be more closer to the real exponential increasing trend, hence, less mismatches or errors when it is used to estimate the aging $\Delta R_{ds,on}$.

In addition, another experiment in [19] which investigates the $\Delta R_{ds,on}$ variation of a device under different stresses is also simulated. The operation is to keep T_m at 180°C, while changing the ΔT_j from 180°C to 140°C at 150 th cycle. The experimental result of the $\Delta R_{ds,on}$ variation from [19]

TABLE 2. Comparison of the N_f cycles among the experimental results, the calculated values and the proposed model with two different aging models respectively.

	ΔT_j	T_m	Calculated N_f	Measured N_f in [19]	Experimental results		Proposed		N_f With Aging $\Delta R_{ds,on}$ =		
					$\alpha 1$	$\beta 1$	$\alpha 2$	β_2	$\alpha_1 e^{\beta_1 t}$	$\alpha_2 e^{\beta_2 t}$	0.05*Q
Case A	160	160	750	200-750	0.313E-3	6.93E-3	1.5E-3	4.67E-3	710	750	715
Case B	140	150	1586	1430	2.413E-3	2.124E-3	1.5E-3	2.21E-3	1430	1593	1480
Case C	130	145	2410	2410	2.696E-3	1.218E-3	1.5E-3	1.453E-3	2410	2390	2350
Case D	80	120	35.2k	20-35k	3.7E-3	8E-5	1.5E-3	9.95E-5	31.5k	35.5k	32k

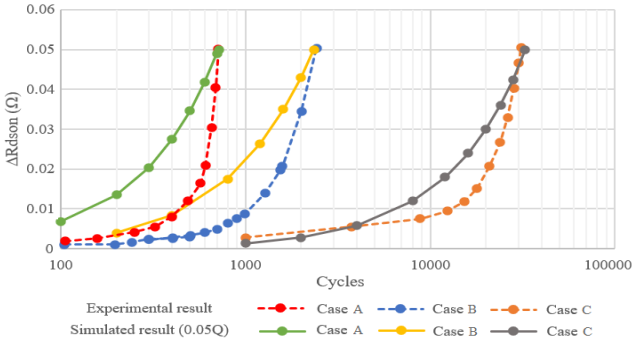

FIGURE 5. A comparison of $\Delta R_{ds,on}$ aging performances between the simulated stress related model and the experimental results of cases (A), (C), and (D).

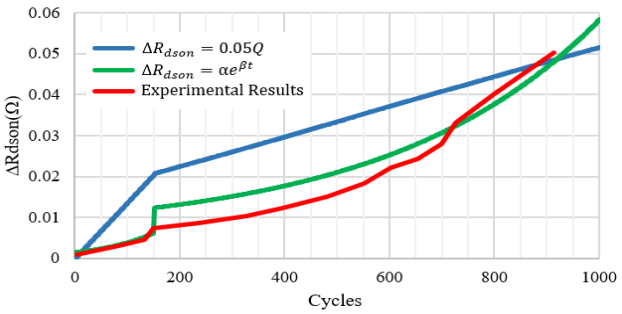

FIGURE 6. Simulation results of the proposed model with exponential and stress related aging models, and experimental results from [19] of $\Delta R_{ds,on}$ resistance variation when ΔT_j is reduced from 180°C to 140°C at 150 cycles with the same $T_m = 180°C$.

and the simulated results of both two models are shown in Fig. 6. As can be seen, to reach the 0.05 ohm limit of $\Delta R_{ds,on}$, the simulated N_f of both two models are close to the experimental result which is 914 cycles, with 930 and 950 cycles for the exponential method and the stress related model respectively. However, in terms of the growing trend, the exponential method gives a better performance. A steep increase occurs at 150th cycle due to the change of load, as the α value for the second load is no longer 0.0015, but will be the accumulated $\Delta R_{ds,on}$ caused by previous load which is around 0.05 in the graph. Since the degradation is irreversible, it is necessary to redefine the initial point. And it also verifies that, the degradation is not only based on the ΔT_j, but also on the device current health state in [14], [15]. While for the stress related method, since it follows the Miner's rule, the $\Delta R_{ds,on}$ increases very fast when under high stresses. The calculated N_f is 371 cycles at $\Delta T_j = 180°C$, hence, at 150 th cycle, the accumulated Q is around 0.4, and the estimated $\Delta R_{ds,on}$ is 0.02 ohm. The growing trend slows down after the load is changed as the stress is lower. This simulation has also validate the point that, a relatively large mismatches can be obtained when use this model to depict high stress thermal cycling experimental results.

To sum up, the exponential model gives a better performance as compared to the stress related model when with high stress thermal cycling mission profiles. However, this advantage will be diminished in long-term lifetime simulation, as the $\Delta R_{ds,on}$ will give more flat aging trend. Both of these two methods can be used in long-term mission profile simulation. In terms of simplicity, the stress related method is adopted and discussed.

B. RANDOM MISSION PROFILE

Fig. 7 gives a complete simulation result of the proposed model with a random mission profile for 120000 seconds (120 Ks) which mimics 10 years load. Fig. 8 gives a close view of a 0.4 Ks simulation results from 11.6 Ks to 12 Ks. The load R_L changes every 5 seconds (5 s) which translates to a change in every 4.8 hours in real life. The ambient temperature profile T_a which includes both annually and daily information is adopted to reflect the device operation environment. Both of these two profiles are periodical and annually based. In the simulation, they are represented by voltage sources V(ta) and V(rl) respectively. The estimated T_j expressed by V(tj_mos) is within the range of 40 °C - 185 °C. As can be seen from Fig. 7, the Q value V(q) reaches 1.1 after 120 Ks, while at 12 Ks in Fig. 8, the value is about 0.077. The lifetime of the device is around 13 years if no aging effects is considered. However, due to the induced degradation feedback loop which accelerates the aging progress, the lifetime is shorter than 13 years, which occurs at 116 Ks (equivalent to 9.67 years). V(rds), which indicates the $R_{ds,on}$ with aging ($R_{init} + \Delta R_{ds,on}$) grows in a similar trend with V(q). While for V(rds_ins), which reflects the aging and temperature dependent real-time $R_{ds,on}$, its values at later 60 Ks are clearly higher than the previous 60 Ks due to the increase of V(rds). V(out) indicates the converter output voltage, due to the open-loop operation, the value varies in the range of 17-21.6 V range. A low V(out) can be found when T_j is high, as the V(rds_ins) is high, more conduction losses are generated.

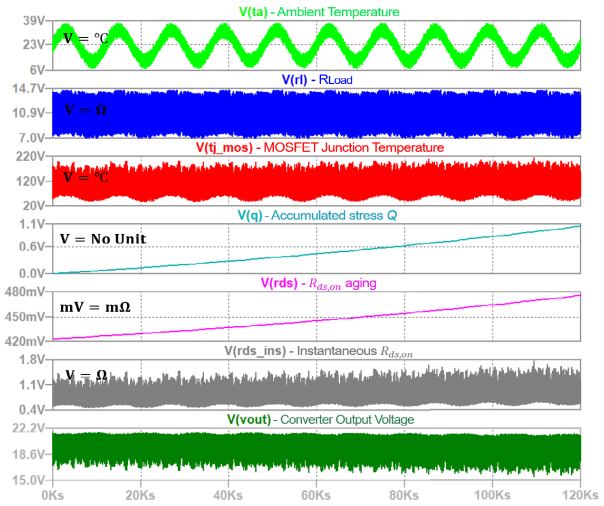

FIGURE 7. An overview of simulation results of a 120 Ks random mission profile with varied ambient temperature to mimic a 10 years converter operation.

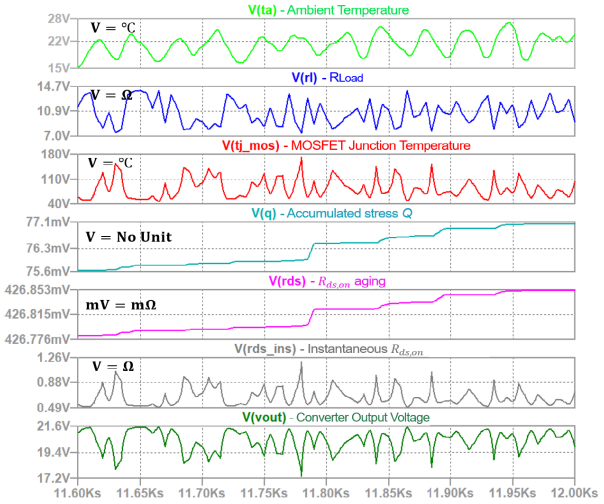

FIGURE 8. A close look of Fig. 7, showing the last 0.4 Ks simulation results from 11.6 Ks to 12 Ks in the first periodical period (12 Ks).

Fig. 9 shows the detailed junction temperature data processing steps. Sample and hold function is used to extract the V(tj_mos) at each load, giving the V(sampling) waveform. Based on it, a continuous comparison between the current temperature value and previous one is made to calculate the difference ΔT_j and the mean temperature T_m and it is fed back to (5). As can be seen from the graph, the accumulation of V(q) remains flat when ΔT_j is low even T_m is high. Meanwhile a steep increase can be observed when ΔT_j is high. Due to the transformation between different domains and adoption of behavioral models, the real unit of each measured waveform has been clarified in Figs. 7-9.

C. SIMULATION SPEED

In this section, the running time of a thermal cycling profile and a long-term profile of the proposed model is compared with a modified MOSFET SPICE model.

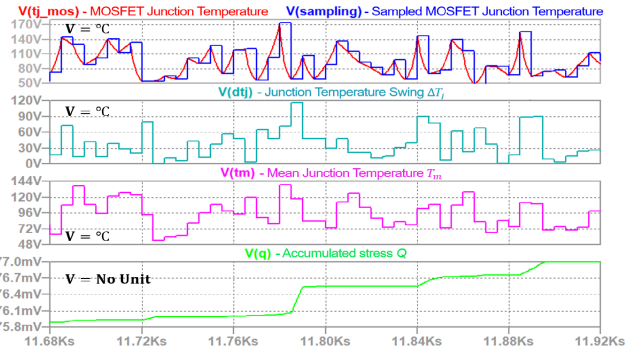

FIGURE 9. T_j data processing stage, including sampling and extraction, T_m and ΔT_j calculation, and Q stress accumulation.

The simulation is completed in a laptop computer, with Inter(R) Core(TM) i7-7600U CPU. The modified MOSFET SPICE model has the same functionality as the proposed model, and the derivation follows similar procedures introduced in this paper. Some minor modifications are made: 1. In the electrical model, an extra resistor is added and connected in series with a normal MOSFET SPICE model representing the increments of $R_{ds,on}$ caused by the temperature and aging; 2. In the thermal model, a foster RC network is used which enables users to see the instantaneous temperature changes. The construction of the electro-thermal model of the modified MOSFET SPICE model can be found in the previous work in [23]. Detailed evaluation and comparison of these two models are given in Table 2.

TABLE 3. A comparison of elapse time of running the thermal cycling simulation and long-term simulation between a switching model and the proposed model.

Simulation tasks	Thermal cycling profile (8 Ks)	Long-term mission profile (5 s)		
Frequency (Hz)	0.1	10 k	20 k	50 k
Elapse time of the switching-model (s)	14.78	819.5	1312.7	3956
Elapse time of the proposed model (s)	12.266	0.145	0.119	0.148

As can be seen, in the 8 Ks high stress thermal cycling simulation, the proposed method does not show significant improvement of simulation speed over the switching model, due to low operation frequency of this mission. However, in the long-term mission profile simulation, with the increase of the switching frequency, the simulation time of the switching model rises dramatically, with 819.5 s, 1312.7 s and 3955.7 s for 10 kHz, 20 kHz and 50 kHz respectively. Meanwhile, the proposed model achieves a relatively constant simulation speed for all three cases and is at least 5600 times faster than switched model. The gap further increases when the switching frequency increases.

IV. DISCUSSION

As the proposed model takes advantage of the ETAM which is independent of frequency, and the switching losses related

terms are add-ons and are represented by equations, this model is well suited for assessing a device which deals with high switching frequency operation, long-term and complex mission profiles. In addition, the precision of the model can be improved by using more accurate equations of such as, switching losses, N_f, and etc. One may argue that this model has not taken parasitic parameters or manufacture settings of the device into consideration. Noted that, the dominant affected parameter in this device is $R_{ds,on}$ from both of the thermal and aging point of view. In addition, the manufacture settings are not easy to be reflected in modeling level, and this scenario happens on the normal MOSFET SPICE model as well. Since devices may differ from one to another, while modeling gives a general information of a device, the common solution to solve it is to use the Weibull analysis to get the time-to-failure probability distribution. Alternatively, for an operating system, online monitoring or prognosis of $R_{ds,on}$ can be implemented to evaluate the device lifetime.

The proposed model allows an instantaneous calculation of the accumulated stress and aging at each half thermal cycle, thanks to the ease of construction of the half-cycle thermal counting algorithm in the circuit simulator. Although it is a widely accepted method, one drawback is that, the accuracy of this algorithm is not as good as rainflow counting method, especially when the device has large temperature fluctuations [20]. Hence, one potential future work is to develop a more accurate thermal counting method in the circuit simulator. Another limitation of this work is that, this model has not considered other failure modes like short circuit, etc. at this stage, which could be considered for future work.

V. CONCLUSION

In this paper, a MOSFET model which merges electro-thermal averaged modeling, aging and lifetime evaluation is proposed in LTspice®, which is a powerful yet freeware circuit simulation tool. Derivation principle of the proposed model are discussed, and two aging descriptive models embedded in it are also investigated and compared. Key features of this work are that, it takes the device aging phenomenon into consideration when estimates its lifetime; secondly, online monitoring of electrical and thermal performances, stress accumulation, degradation and lifetime consumption can be realized simultaneously, which are achieved by using thermal-electrical analogy and behavioral models. High stress thermal cycling simulation is implemented for verification purpose. The results show an agreement with [19]. While for the long-term load simulation, an accelerated degradation progress can be observed due to the accumulated stress on device. The estimated lifetime with and without inducing aging effects are equivalent to 9.67 and 13 years respectively. Thus, it is important to consider aging when evaluating device lifetime. Another benefit of the model is the fast simulation speed due to ETAM, allowing a 120 Ks simulation to be completed in around 46 s. Hence, the model has high potential for long-term lifetime evaluation of circuit device.

REFERENCES

[1] S. Dusmez and B. Akin, "An accelerated thermal aging platform to monitor fault precursor on-state resistance," in *Proc. IEEE Int. Electric Mach. Drives Conf. (IEMDC)*, May 2015, pp. 1352–1358.

[2] A. Testa, S. De Caro, and S. Russo, "A reliability model for power MOSFETs working in avalanche mode based on an experimental temperature distribution analysis," *IEEE Trans. Power Electron.*, vol. 27, no. 6, pp. 3093–3100, Jun. 2012.

[3] L. Ceccarelli, R. M. Kotecha, A. S. Bahman, F. Iannuzzo, and H. A. Mantooth, "Mission-profile-based lifetime prediction for a SiC MOSFET power module using a multi-step condition-mapping simulation strategy," *IEEE Trans. Power Electron.*, vol. 34, no. 10, pp. 9698–9708, Oct. 2019.

[4] P. Diaz Reigosa, H. Wang, Y. Yang, and F. Blaabjerg, "Prediction of bond wire fatigue of IGBTs in a PV inverter under a long-term operation," *IEEE Trans. Power Electron.*, vol. 31, no. 10, pp. 7171–7182, Oct. 2016.

[5] J. He, A. Sangwongwanich, Y. Yang, and F. Iannuzzo, "Lifetime evaluation of power modules for three-level 1500-V photovoltaic inverters," in *Proc. IEEE Appl. Power Electron. Conf. Expo. (APEC)*, Mar. 2020, pp. 430–435.

[6] A. Sangwongwanich, Y. Yang, D. Sera, and F. Blaabjerg, "Lifetime evaluation of grid-connected PV inverters considering panel degradation rates and installation sites," *IEEE Trans. Power Electron.*, vol. 33, no. 2, pp. 1225–1236, Feb. 2018.

[7] Y. Shen, A. Chub, H. Wang, D. Vinnikov, E. Liivik, and F. Blaabjerg, "Wear-out failure analysis of an impedance-source PV microinverter based on system-level electrothermal modeling," *IEEE Trans. Ind. Electron.*, vol. 66, no. 5, pp. 3914–3927, May 2019.

[8] H. Liu, K. Ma, Z. Qin, P. C. Loh, and F. Blaabjerg, "Lifetime estimation of MMC for offshore wind power HVDC application," *IEEE J. Emerg. Sel. Topics Power Electron.*, vol. 4, no. 2, pp. 504–511, Jun. 2016.

[9] K. Ma, M. Liserre, F. Blaabjerg, and T. Kerekes, "Thermal loading and lifetime estimation for power device considering mission profiles in wind power converter," *IEEE Trans. Power Electron.*, vol. 30, no. 2, pp. 590–602, Feb. 2015.

[10] U. Shipurkar, E. Lyrakis, K. Ma, H. Polinder, and J. A. Ferreira, "Lifetime comparison of power semiconductors in three-level converters for 10-MW wind turbine systems," *IEEE J. Emerg. Sel. Topics Power Electron.*, vol. 6, no. 3, pp. 1366–1377, Sep. 2018.

[11] H. Huang and P. A. Mawby, "A lifetime estimation technique for voltage source inverters," *IEEE Trans. Power Electron.*, vol. 28, no. 8, pp. 4113–4119, Aug. 2013.

[12] M. Musallam, C. Yin, C. Bailey, and M. Johnson, "Mission profile-based reliability design and real-time life consumption estimation in power electronics," *IEEE Trans. Power Electron.*, vol. 30, no. 5, pp. 2601–2613, May 2015.

[13] Z. Chen, F. Gao, C. Yang, T. Peng, L. Zhou, and C. Yang, "Converter lifetime modeling based on online rainflow counting algorithm," in *Proc. IEEE 28th Int. Symp. Ind. Electron. (ISIE)*, Jun. 2019, pp. 1743–1748.

[14] W. Lai, M. Chen, L. Ran, S. Xu, N. Jiang, X. Wang, O. Alatise, and P. Mawby, "Experimental investigation on the effects of narrow junction temperature cycles on die-attach solder layer in an IGBT module," *IEEE Trans. Power Electron.*, vol. 32, no. 2, pp. 1431–1441, Feb. 2017.

[15] W. Lai, M. Chen, L. Ran, O. Alatise, S. Xu, and P. Mawby, "Low stress cycle effect in IGBT power module die-attach lifetime modeling," *IEEE Trans. Power Electron.*, vol. 31, no. 9, pp. 6575–6585, Sep. 2016.

[16] W. Lai, Y. Zhao, M. Chen, Y. Wang, X. Ding, S. Xu, and L. Pan, "Condition monitoring in a power module using on-state resistance and case temperature," *IEEE Access*, vol. 6, pp. 67108–67117, 2018.

[17] T. Cheng, D. Dah-ChuanLu, and Y. P. Siwakoti, "Electro-thermal average modeling of a boost converter considering device self-heating," in *Proc. IEEE Appl. Power Electron. Conf. Expo. (APEC)*, Mar. 2020, pp. 2854–2859.

[18] *LTspice B Sources (Complete Reference)*. Accessed: Nov. 2019. [Online]. Available: http://ltwiki.org/index.php?title=B_sources_complete_reference

[19] S. Dusmez, H. Duran, and B. Akin, "Remaining useful lifetime estimation for thermally stressed power MOSFETs based on on-state resistance variation," *IEEE Trans. Ind. Appl.*, vol. 52, no. 3, pp. 2554–2563, May 2016.

[20] K. Mainka, M. Thoben, and O. Schilling, "Lifetime calculation for power modules, application and theory of models and counting methods," in *Proc. 14th Eur. Conf. Power Electron. Appl.*, Birmingham, U.K., 2011, pp. 1–8.

[21] W. Lai, P. A. Mawby, H. Qin, O. Alatise, S. Xu, M. Chen, and L. Ran, "Study on the lifetime characteristics of power modules under power cycling conditions," *IET Power Electron.*, vol. 9, no. 5, pp. 1045–1052, Apr. 2016.
[22] S. Dusmez, M. Heydarzadeh, M. Nourani, and B. Akin, "Remaining useful lifetime estimation for power MOSFETs under thermal stress with RANSAC outlier removal," *IEEE Trans. Ind. Informat.*, vol. 13, no. 3, pp. 1271–1279, Jun. 2017.
[23] T. Cheng, D. D.-C. Lu, and Y. Siwakoti, "Electro-thermal modeling of a boost converter considering device self-heating," in *Proc. IEEE 4th Int. Future Energy Electron. Conf. (IFEEC)*, Nov. 2019, pp. 1–6.

TIAN CHENG (Student Member, IEEE) received the B.Eng. and M.Phil. degrees in electrical engineering from The University of Sydney, Australia, in 2014 and 2017, respectively, where she is currently pursuing the Ph.D. degree in power electronics. Her current research interests include modeling of power semiconductor devices and converters, and reliability of power electronics.

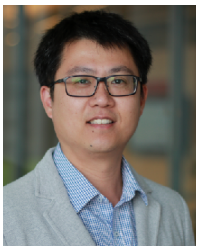

DYLAN DAH-CHUAN LU (Senior Member, IEEE) received the Ph.D. degree in electronic and information engineering from The Hong Kong Polytechnic University, Hong Kong, in 2004. He joined Power^{e}Lab Ltd., in 2003, as a Senior Design Engineer, where he was responsible for industrial switching power supply projects. From 2006 to 2016, he was a full-time Faculty Member with The University of Sydney, Australia, where he now holds an honorary position. He joined University of Technology Sydney, Australia, in July 2016, where he is currently a Professor and the Head of Discipline of Electrical Power and Energy Systems with the School of Electrical and Data Engineering. He has authored or coauthored more than 100 international journals and held two patents in power electronics. His current research interests include efficient, cost-effective and reliable power conversion for renewable energy sources, energy storage systems, and microgrids. He is currently serving as the Chair for the Joint Chapter IAS/IES/PELS (IEEE New South Wales Section) and an Associate Editor for the IEEE TRANSACTIONS ON INDUSTRIAL ELECTRONICS.

YAM P. SIWAKOTI (Senior Member, IEEE) received the B.Tech. degree in electrical engineering from the National Institute of Technology, Hamirpur, India, in 2005, the joint M.E. degree in electrical power engineering from the Norwegian University of Science and Technology, Trondheim, Norway, and from Kathmandu University, Dhulikhel, Nepal, in 2010, and the Ph.D. degree in electronic engineering from Macquarie University, Sydney, Australia, in 2014.

From 2014 to 2016, he was a Postdoctoral Fellow with the Department of Energy Technology, Aalborg University, Denmark. From 2017 to 2018, he was a Visiting Scientist with the Fraunhofer Institute for Solar Energy Systems, Freiburg, Germany. He is currently a Senior Lecturer with the Faculty of Engineering and Information Technology, University of Technology Sydney, Australia.

Dr. Siwakoti was a recipient of the prestigious Green Talent Award from the Federal Ministry of Education and Research, Germany, in 2016. He serves as an Associate Editor for three major journals of IEEE (IEEE TRANSACTIONS ON POWER ELECTRONICS, IEEE TRANSACTIONS ON INDUSTRIAL ELECTRONICS, IEEE JOURNAL OF EMERGING AND SELECTED TOPICS IN POWER ELECTRONICS), and the *IET Power Electronics*.